

Science**Direct Observation of the Three-State Folding of a Single Protein Molecule**Ciro Cecconi, *et al.**Science* **309**, 2057 (2005);

DOI: 10.1126/science.11116702

The following resources related to this article are available online at www.sciencemag.org (this information is current as of October 15, 2008):

Updated information and services, including high-resolution figures, can be found in the online version of this article at:

<http://www.sciencemag.org/cgi/content/full/309/5743/2057>

Supporting Online Material can be found at:

<http://www.sciencemag.org/cgi/content/full/309/5743/2057/DC1>

This article **cites 27 articles**, 6 of which can be accessed for free:

<http://www.sciencemag.org/cgi/content/full/309/5743/2057#otherarticles>

This article has been **cited by** 71 article(s) on the ISI Web of Science.

This article has been **cited by** 21 articles hosted by HighWire Press; see:

<http://www.sciencemag.org/cgi/content/full/309/5743/2057#otherarticles>

This article appears in the following **subject collections**:

Biochemistry

<http://www.sciencemag.org/cgi/collection/biochem>

Information about obtaining **reprints** of this article or about obtaining **permission to reproduce this article** in whole or in part can be found at:

<http://www.sciencemag.org/about/permissions.dtl>

3. P. Castelo-Branco *et al.*, *Mol. Cell. Biol.* **24**, 4174 (2004).
4. K. P. Knoch *et al.*, *Nat. Cell Biol.* **6**, 207 (2004).
5. B. Amir-Ahmady, P. L. Boutz, V. Markovstov, M. Phillips, D. L. Black, *RNA* **11**, 699 (2005).
6. H. Liu, W. Zhang, R. B. Reed, W. Liu, P. J. Grabowski, *RNA* **8**, 137 (2002).
7. J. M. Izquierdo *et al.*, *Mol. Cell* **19**, 475 (2005).
8. S. Sharma, A. Falick, D. Black, *Mol. Cell* **19**, 485 (2005).
9. C. Maris, C. Dominguez, F. H. T. Allain, *FEBS J.* **272**, 2118 (2005).
10. P. J. Simpson *et al.*, *Structure* **12**, 1631 (2004).
11. M. R. Conte *et al.*, *EMBO J.* **19**, 3132 (2000).
12. I. Perez, C. H. Lin, J. G. McAfee, J. G. Patton, *RNA* **3**, 764 (1997).
13. R. Singh, J. Valcarcel, M. R. Green, *Science* **268**, 1173 (1995).
14. R. C. Chan, D. L. Black, *Mol. Cell. Biol.* **15**, 6377 (1995).
15. R. C. Chan, D. L. Black, *Mol. Cell. Biol.* **17**, 4667 (1997).
16. Additional results, materials, and methods are available as supporting material on Science Online.
17. R. F. Roscigno, M. Weiner, M. A. Garcia-Blanco, *J. Biol. Chem.* **268**, 11222 (1993).
18. N. Gromak *et al.*, *EMBO J.* **22**, 6356 (2003).
19. R. C. Deo, J. B. Bonanno, N. Sonenberg, S. K. Burley, *Cell* **98**, 835 (1999).
20. N. Handa *et al.*, *Nature* **398**, 579 (1999).
21. F. H. Allain, P. Bouvet, T. Dieckmann, J. Feigon, *EMBO J.* **19**, 6870 (2000).
22. H. Shen, J. L. Kan, C. Ghigna, G. Biamonti, M. R. Green, *RNA* **10**, 787 (2004).
23. C. Gooding, G. C. Roberts, G. Moreau, B. Nadal-Ginard, C. W. Smith, *EMBO J.* **13**, 3861 (1994).
24. J. Southby, C. Gooding, C. W. Smith, *Mol. Cell. Biol.* **19**, 2699 (1999).
25. E. J. Wagner, M. A. Garcia-Blanco, *Mol. Cell* **10**, 943 (2002).
26. H. Lou, D. M. Helfman, R. F. Gagel, S. M. Berget, *Mol. Cell. Biol.* **19**, 78 (1999).
27. N. Charlet-B., P. Logan, G. Singh, T. A. Cooper, *Mol. Cell* **9**, 649 (2002).
28. M. Ashiya, P. J. Grabowski, *RNA* **3**, 996 (1997).
29. N. Gromak, A. J. Matlin, T. A. Cooper, C. W. Smith, *RNA* **9**, 443 (2003).
30. C. Gooding, G. C. Roberts, C. W. Smith, *RNA* **4**, 85 (1998).
31. R. P. Carstens, E. J. Wagner, M. A. Garcia-Blanco, *Mol. Cell. Biol.* **20**, 7388 (2000).
32. E. V. Pilipenko *et al.*, *Genes Dev.* **14**, 2028 (2000).
33. S. A. Mitchell, K. A. Spriggs, M. J. Coldwell, R. J. Jackson, A. E. Willis, *Mol. Cell* **11**, 757 (2003).
34. M. Y. Chou, J. G. Underwood, J. Nikolic, M. H. Luu, D. L. Black, *Mol. Cell* **5**, 949 (2000).
35. We are grateful to R. Stefl (ETH Zürich) for help with

the structure calculation and to L. Skrisovska, C. Maris, and G. Wider (ETH Zürich), S. Curry, and S. Matthews (Imperial College, London) for helpful discussions. We also thank R. Peterson and J. Feigon (UCLA) for sharing recently developed NMR pulse programs. This investigation was supported by grants from the Swiss National Science Foundation, the Structural Biology National Center of Competence in Research to S.P. and F.H.T.A. and by the Roche Research Fund for Biology at ETH Zürich to F.H.T.A. F.H.T.A. is a European Molecular Biology Organization Young Investigator. The coordinates of the structures of PTB RBD1, RBD2, and RBD34 in complex with CUCUCU have been deposited in the Protein Data Bank with accession codes 2AD9, 2ADB, and 2ADC, respectively.

Supporting Online Material

www.sciencemag.org/cgi/content/full/309/5743/2054/DC1

Materials and Methods

SOM Text

Figs. S1 to S4

Table S1

References

26 April 2005; accepted 24 August 2005
10.1126/science.1114066

Direct Observation of the Three-State Folding of a Single Protein Molecule

Ciro Cecconi,^{1,2*} Elizabeth A. Shank,^{1*} Carlos Bustamante,^{1,2,3†}
Susan Marqusee^{1†}

We used force-measuring optical tweezers to induce complete mechanical unfolding and refolding of individual *Escherichia coli* ribonuclease H (RNase H) molecules. The protein unfolds in a two-state manner and refolds through an intermediate that correlates with the transient molten globule-like intermediate observed in bulk studies. This intermediate displays unusual mechanical compliance and unfolds at substantially lower forces than the native state. In a narrow range of forces, the molecule hops between the unfolded and intermediate states in real time. Occasionally, hopping was observed to stop as the molecule crossed the folding barrier directly from the intermediate, demonstrating that the intermediate is on-pathway. These studies allow us to map the energy landscape of RNase H.

Protein folding remains a major unsolved challenge for modern molecular biology. Theoretical studies emphasize the potential heterogeneous nature of the process; however, traditional bulk biochemical experiments often mask this complexity in their inherent ensemble averaging. For instance, many proteins are observed to populate partially structured conformations early during the folding process (1, 2). These so-called burst-phase intermediates (I) are often formed within the dead time of

the measuring instrument (usually milliseconds) and therefore cannot be characterized directly. Thus, controversy remains about whether these intermediates are on-pathway and productive to protein folding, or are off-pathway and do not lead directly to the folded state (2, 3). It is also unclear whether these intermediates constitute distinct thermodynamic states or simply represent a redistribution of the unfolded ensemble when exposed to native conditions (4). These issues can be addressed with the use of single-molecule manipulation to follow in real time the trajectories of individual protein molecules during mechanically induced unfolding/refolding processes.

Previous single-molecule manipulation studies have used the atomic force microscope (AFM) to characterize the mechanical unfolding and refolding of tandem repeats of globular protein domains (5–11). Although informative,

this approach has been limited to characterizing the high-force unfolding behavior of proteins. It has been difficult to observe the refolding process directly or to monitor the equilibrium between the folded and unfolded states using this method, in part because of the high spring constants of commercially available cantilevers and the correspondingly high loading rates they exert. In contrast, optical tweezers, with considerably reduced mechanical stiffness and loading rates, can overcome these limitations, as shown in RNA unfolding studies (12). Optical tweezers have been used to mechanically unfold the multiglobular protein titin (5, 13); although the resulting data revealed the overall mechanical unfolding response of the molecule, the heterogeneous composition of this protein obscured the unfolding of the individual globular domains and refolding could not be observed directly.

Here, we report the complete force-induced unfolding and refolding trajectory of a single molecule of the *E. coli* protein ribonuclease H* Q4C/V155C (14) (referred to herein as RNase H) with the use of force-measuring optical tweezers (15). RNase H is a 155-residue, single-domain protein whose structure, stability, and folding mechanism have been extensively characterized using bulk biochemical techniques. The central portion of the polypeptide forms the core of the protein (Fig. 1A), being both the first region to fold (16) and the most stable region of the native structure (17). This observation and additional kinetic and mutagenesis studies support the hypothesis that RNase H folds via a hierarchical mechanism, in which the most stable regions of the native structure form first during folding (3, 18). It has been impossible, however, to demonstrate this behavior directly with traditional approaches. This wealth of both equilibrium

¹Department of Molecular and Cell Biology and Institute for Quantitative Biology, ²Department of Physics, ³Howard Hughes Medical Institute, University of California, Berkeley, CA 94720, USA.

*These authors contributed equally to this work.

†To whom correspondence should be addressed. E-mail: carlos@alice.berkeley.edu; marqusee@berkeley.edu

and kinetic data makes RNase H an ideal model system to explore single-molecule protein folding trajectories and the nature of protein folding intermediates.

We used two ~500-base pair double-stranded DNA molecules to tether individual RNase H molecules between two polystyrene spheres ~2 μm in diameter (Fig. 1A) (19). These “molecular handles,” attached to the protein through unique engineered cysteine residues, function as spacers to prevent non-specific bead-bead interactions and permit manipulation of the ~3 nm diameter protein. RNase H is folded and retains activity when attached to DNA handles (fig. S1). By moving the bead on the pipette relative to the bead in the trap, each RNase H molecule was stretched and relaxed multiple times, generating force-extension curves (Fig. 1B) (20). We observed sudden changes in extension of the molecule (transitions) during both stretching and relaxation, corresponding to the unfolding and refolding of the protein. These transitions were not observed during control experiments with DNA handles alone (yellow trace, Fig. 1B). Unfolding transitions occurred at two distinct forces, ~19 pN or ~5.5 pN, whereas the refolding transitions exhibited a single narrow distribution centered at ~5.5 pN, coincident with the lower of the two unfolding transition forces (fig. S2).

The increment in contour length (ΔL_c) corresponding to each transition was estimated by fitting the force-extension curves with the worm-like chain model (21). The high-force transitions at ~19 pN were consistent with the complete unfolding of RNase H (ΔL_c of 50 ± 5 nm versus 50.4 nm calculated for the full-

length protein). In contrast, the ΔL_c obtained from the low-force unfolding (39 ± 6 nm) and refolding transitions (40 ± 10 nm) imply that the associated conformational changes involve a smaller portion of the polypeptide chain. Indeed, close inspection of the force-extension curves reveals that the refolding transition does not restore the original length of the molecule, leaving a gap between the stretching and relaxation curves at ~5.5 pN (Fig. 1B) and supporting the idea of partial refolding. Together, these data indicate that the native RNase H structure completely unfolds at ~19 pN (N, native → U, unfolded), and then, upon return to ~5.5 pN, partially refolds into an intermediate structure (U → I). The refolding intermediate unfolds again at ~5.5 pN in the next stretching cycle, unless the relaxed protein is incubated for a time sufficient to fully refold (I → N) before being stretched again.

We therefore monitored whether the protein had fully refolded into its native structure by examining subsequent stretching curves for the presence of a high-force unfolding transition. The probability that the intermediate folds into the native state between successive cycles while held at force F for a period of time t is given by

$$P_f(F, t) = 1 - \exp\{-tk_{\text{obs}(I \rightarrow N)} \exp[-(F\Delta x_{I \rightarrow N}^\ddagger/k_B T)]\} \quad (1)$$

(22), where $\Delta x_{I \rightarrow N}^\ddagger$ is the distance from the intermediate to the transition state, $k_{\text{obs}(I \rightarrow N)} = k_m k_{I \rightarrow N}^o$ [where k_m reflects any possible contribution of the instrument to the overall refolding rate (12) and $k_{I \rightarrow N}^o$ is the rate of

the I → N transition at zero force], and $k_B T$ is the product of the Boltzmann constant and absolute temperature. The probability of the I → N transition was determined as a function of force and incubation time, and the data were fit with a linearized form of Eq. 1 (Fig. 2A), yielding $k_{\text{obs}(I \rightarrow N)} = 0.17 \pm 0.03 \text{ s}^{-1}$ and $\Delta x_{I \rightarrow N}^\ddagger = 1.5 \pm 0.3 \text{ nm}$. Bulk studies on RNase H have also revealed a transient folding intermediate with a similar refolding rate ($k_{I \rightarrow N(\text{bulk})} = 0.74 \pm 0.02 \text{ s}^{-1}$) (16).

The hysteresis observed between the unfolding of the native state (N → U) and the refolding transitions suggests that the rate of pulling in these experiments is faster than the rate at which these states can equilibrate under these conditions. By pulling the molecule at different loading rates, the observed unfolding rate of the molecule at zero force is found to

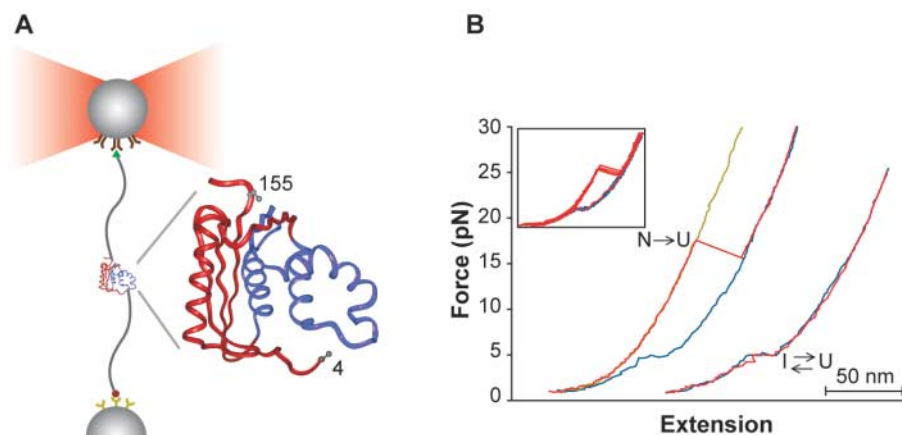


Fig. 1. Experimental setup and RNase H force-extension curves. (A) RNase H contains two unique cysteines at positions 4 and 155 (ball-and-stick model) that allow attachment to the DNA handles. The region of RNase H shown in blue comprises the intermediate identified in bulk studies: the core, or most stable region of the protein, as well as the portion formed earliest during folding (16, 17).

The sample was tethered to functionalized beads with the use of the digoxigenin and biotin moieties present at the distal ends of the handles. One bead is held in place at the end of a micropipette by suction, the other by the optical trap. (B) Stretching (red) and relaxation (blue) force-extension curves from RNase H display high- and low-force unfolding transitions. Refolding transitions were observed at the same forces as the low-force unfolding. A force-extension curve from DNA alone is shown in yellow. Inset shows curves from sequential pulling cycles.

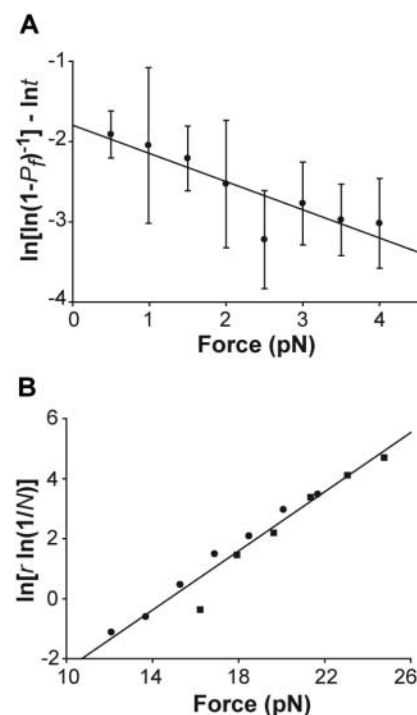


Fig. 2. Refolding probability and unfolding distribution of the native state of RNase H. (A) The probability of refolding from I to N (P_f) as a function of force (F) and time (t) was fit to

$$\ln \left[\ln \left(\frac{1}{1 - P_f} \right) \right] - \ln t = \ln k_{\text{obs}(I \rightarrow N)} - \frac{F\Delta x_{I \rightarrow N}^\ddagger}{k_B T}$$

yielding the best fit (least squares) values of $k_{\text{obs}(I \rightarrow N)} = 0.17 \pm 0.03 \text{ s}^{-1}$ and $\Delta x_{I \rightarrow N}^\ddagger = 1.5 \pm 0.3 \text{ nm}$. The error bars are the standard deviations of the data from various refolding times at those forces. (B) Force distribution of the native structure unfolding at a loading rate of 13 pN s^{-1} (solid circles) and 53 pN s^{-1} (solid squares), where r is the loading rate and N is the fraction of folded protein (12). The best fit (least squares) values are $k_{\text{obs}(N \rightarrow U)} = 3 (\pm 2) \times 10^{-4} \text{ s}^{-1}$ and $\Delta x_{N \rightarrow U}^\ddagger = 2.0 \pm 0.1 \text{ nm}$.

be $k_{\text{obs}(N \rightarrow U)} = 3 (\pm 2) \times 10^{-4} \text{ s}^{-1}$, and the distance between the native state and the first transition state is $\Delta x_{N \rightarrow U}^\ddagger = 2.0 \pm 0.1 \text{ nm}$ (Fig. 2B) (23) when analyzed in a manner analogous to that used in previous AFM studies (24). This value of $k_{\text{obs}(N \rightarrow U)}$ corresponds well with the $k_{(N \rightarrow U)(\text{bulk})}$ value, $1.7 (\pm 0.04) \times 10^{-5} \text{ s}^{-1}$ (16).

In contrast to the hysteresis observed for the $N \rightarrow U$ transition, the unfolding and refolding transitions of the mechanical refolding intermediate ($I \rightarrow U$ and $U \rightarrow I$) coincide (Fig. 1B), indicating that this process occurs reversibly under the experimental conditions used here (fig. S3). Consistent with this observation, the force-extension curves occasionally displayed rapid fluctuations in extension near 5.5 pN rather than a single sharp transition (fig. S4). We examined this behavior further by relaxing the unfolded protein and holding the polypeptide at a fixed force with the use of the instrument's force-

feedback mode (12). When held at a force near 5.5 pN, the RNase H molecule displayed bistability: The molecule “hopped” between the intermediate and the denatured form of the protein in real time, with the molecular extension shifting rapidly by $15 \pm 4 \text{ nm}$ (Fig. 3A). Changing the set point of the force altered this equilibrium between the extended unfolded state and the compact intermediate structure (Fig. 3A). Such hopping has also been seen for a simple RNA hairpin using a similar approach (12), and for a chemically destabilized two-state ($U \rightleftharpoons N$) protein monitored for short time periods by fluorescence resonance energy transfer (25). We now show the extended real-time equilibrium behavior of a complex globular protein.

The force-dependent rates of unfolding and refolding of the intermediate were determined from the lifetimes of the extended (U) and compact (I) states seen in the hopping experiments. The position of the transition

state between I and U was then estimated by fitting the rates to the Arrhenius-like equation

$$k_{I \rightarrow U} = k_m k_{I \rightarrow U}^0 \exp(F \Delta x_{I \rightarrow U}^\ddagger / k_B T) \quad (2)$$

where $k_{I \rightarrow U}^0$ is the unfolding rate at zero force, and $\Delta x_{I \rightarrow U}^\ddagger$ is the distance from I to the transition state along the reaction coordinate (12). A similar analysis holds true for the reverse $U \rightarrow I$ reaction. The slopes of plots of $\ln k$ versus force yielded $\Delta x_{I \rightarrow U}^\ddagger = 5 \pm 1 \text{ nm}$ and $\Delta x_{U \rightarrow I}^\ddagger = 6 \pm 1 \text{ nm}$. These values are substantially larger than those found for the native-state unfolding ($\Delta x_{N \rightarrow U}^\ddagger$) of several other proteins using the AFM (26). Our results on RNase H therefore convey a picture of the intermediate as a pliable structure that can deform elastically a great amount before the reaction is committed to unfolding. Such large transition-state distances have been observed in other biomolecules and were interpreted as reflecting the mechanical behavior of structures lacking the nonlocal specific contacts associated with tertiary interactions from the intermediate to its transition state and the low forces required to unfold it suggest that this structure is only able to form weak, possibly transient tertiary interactions, and that it therefore resembles a molten globule structure (27).

We evaluated the thermodynamics of the $U \rightleftharpoons I$ transition ($\Delta G_{(UI)}$) with three independent methods (Fig. 3B). We measured the area under the refolding plateau in the force-extension curves, calculated the force-dependent equilibrium constant between U and I, and analyzed the transitions with the statistics of a two-state system. After correcting for the entropy loss due to tethering and stretching the U state [calculated to be $5.1 \pm 0.6 \text{ kcal/mol}$ (19)], we obtained $\Delta G_{(UI)} = 4 \pm 3 \text{ kcal/mol}$, $4 \pm 2 \text{ kcal/mol}$, and $3.8 \pm 0.8 \text{ kcal/mol}$, respectively. The agreement between these free energy values validates the analyses. The remarkable similarity between these values and that observed in ensemble experiments ($\Delta G_{(UI)(\text{bulk})} = 3.6 \pm 0.1 \text{ kcal/mol}$), in conjunction with the similar refolding kinetics ($k_{I \rightarrow N}$), suggests that the intermediate detected in our single-molecule mechanical manipulations correlates with that sampled in solution. To further probe this relationship, we performed similar optical tweezer experiments using a variant of RNase H (I53D) that displays two-state folding in solution (28). In this case we saw no evidence of an intermediate (Fig. 3C) (29). These results strongly suggest that the intermediate observed in our single-molecule experiments is similar to that detected by ensemble methods, and hence the new features found in this study are relevant to the folding process in solution.

In the ensemble refolding experiments of RNase H, the formation of I occurs very

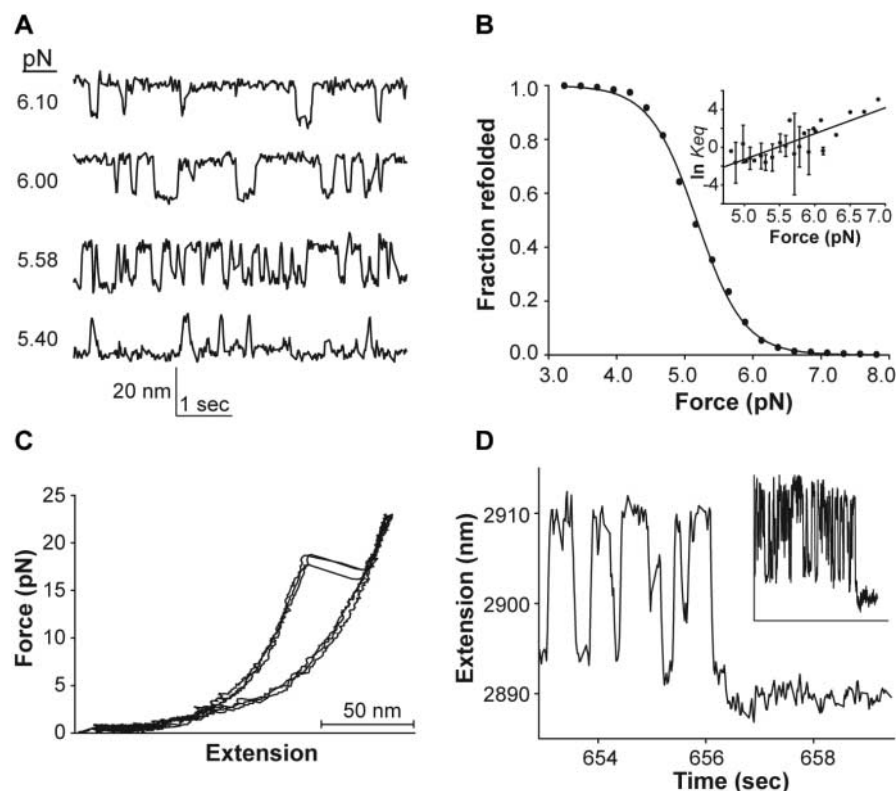


Fig. 3. Characterization of the folding intermediate of RNase H. (A) Extension versus time traces for RNase H at various constant forces. (B) The probability of U refolding to I as a function of force was obtained from a normalized frequency histogram of refolding forces ($n = 664$). The solid line shows the probability, $P(E)$, of a two-state system (12). The best fit (least squares) values are $\Delta G_{(UI)} = 8.9 \pm 0.3 \text{ kcal/mol}$ and $\Delta x_{(UI)} = 11.9 \pm 0.3 \text{ nm}$. Inset shows the equilibrium constant (K_{eq}) of the $U \rightleftharpoons I$ transition at any given force, obtained from the ratio of the lifetimes of the I and U states. Fitting the plot of $\ln K_{\text{eq}}$ versus force yielded the best fit (least squares) values of $\Delta G_{(UI)} = 9 \pm 2 \text{ kcal/mol}$ and $\Delta x_{(UI)} = 11 \pm 2 \text{ nm}$ (12, 19). Data within 0.024 pN were grouped; error bars are the standard deviations of the data. Measuring the area under the unfolding/refolding plateau (potential of mean force) yielded a $\Delta G_{(UI)}$ of $9 \pm 2 \text{ kcal/mol}$ and $\Delta x_{(UI)} = 12 \pm 3 \text{ nm}$ (not shown). (C) Force-extension curves for the I53D RNase H variant (compare to curves in Fig. 1B). Unlike RNase H, the I53D variant does not show low-force refolding or unfolding transitions. (D) Length versus time trace of RNase H. Hopping stops when the protein refolds to the native state. Inset shows a longer time trace.

rapidly (within the 12-ms dead time of the stopped-flow instrument) and is therefore not observed directly (16). It has thus been impossible to determine unambiguously whether this kinetic intermediate is a distinct thermodynamic state or simply the result of a shift in the population of a continuum of unfolded states. Both models have been suggested from experimental and theoretical studies (4). In our studies, we used force to modulate the equilibrium between the U and I states until the interconversion between these two forms became observable. Our data clearly indicate that the transition between the I and U states is first-order (Fig. 3A) (fig. S5), allowing us to directly characterize the kinetic, thermodynamic, and mechanical properties of this molten globule-like state. The forces holding together the intermediate are small but still substantial (~5.5 pN), amounting to about one-third of the forces that stabilize the fully folded state at the pulling rates used in our experiments. The magnitude of these forces, the sharpness of their distribution, and the first-order nature of the transition from and to the unfolded state clearly indicate that this molten globule-like

intermediate is a well-defined, thermodynamically distinct stable molecular form held together by distinct, although not necessarily specific, interactions.

Sometimes during constant force experiments, the hopping corresponding to the $U \rightleftharpoons I$ transition spontaneously ceased. An additional compaction always preceded the termination of hopping (Fig. 3D). The size of this compaction, as estimated from the worm-like chain model, corresponds well to that expected for the $I \rightarrow N$ transition at the given force. Indeed, stretching the molecule after hopping ceased invariably resulted in a high-force unfolding transition (~19 pN), as expected for the unfolding of the native state. Thus, it was possible to observe the $I \rightarrow N$ transition directly. In 78% of the traces ($n = 18$) in which hopping stopped, the transition to the native state clearly took place from the folded intermediate structure, as in Fig. 3D. In the rest of the cases, the time spent in I before the transition to N may have been too short to be resolved in our experiments. These data indicate that the refolding intermediate observed in our experiments exists on-pathway to the folded state. Furthermore, the fact that the $U \rightarrow I$ transition is invariably present in our force-relaxation curves indicates that the same intermediate is also an obligatory step in the folding trajectory of RNase H (Fig. 4A).

The ability to explore the behavior of single protein molecules with the use of optical tweezers has permitted us to map the energy landscape traversed by the small globular protein RNase H in its transitions to and from its unfolded state (Fig. 4B). Our observation of a folding intermediate that corresponds to the intermediate seen in bulk suggests that both methods probe the same fundamental barriers. The new features revealed in this study therefore enhance our understanding of how proteins fold in solution. The intermediate of RNase H forms a distinct thermodynamic state that, although compact and held together by cohesive interactions, is nonetheless highly deformable. This state appears to be both on-pathway and obligatory to the folding trajectory.

10. M. Carrion-Vazquez *et al.*, *Nat. Struct. Biol.* **10**, 738 (2003).
11. J. M. Fernandez, H. Li, *Science* **303**, 1674 (2004).
12. J. Liphardt, B. Onoa, S. B. Smith, I. J. Tinoco, C. Bustamante, *Science* **292**, 733 (2001).
13. M. S. Kellermayer, S. B. Smith, C. Bustamante, H. L. Granzier, *J. Struct. Biol.* **122**, 197 (1998).
14. J. M. Dabora, S. Marqusee, *Protein Sci.* **3**, 1401 (1994).
15. S. B. Smith, Y. Cui, C. Bustamante, *Methods Enzymol.* **361**, 134 (2003).
16. T. M. Raschke, S. Marqusee, *Nat. Struct. Biol.* **4**, 298 (1997).
17. A. K. Chamberlain, T. M. Handel, S. Marqusee, *Nat. Struct. Biol.* **3**, 782 (1996).
18. T. M. Raschke, J. Kho, S. Marqusee, *Nat. Struct. Biol.* **6**, 825 (1999).
19. See supporting data on Science Online.
20. Single-molecule tethers were recognized by identifying the overstretching transition due to the DNA handles. Only those fibers that exhibited an overstretching transition of the expected length (~230 nm) at the correct force (~67 pN) for a single fiber containing 1116-base pair DNA were selected for analysis.
21. J. F. Marko, E. D. Siggia, *Macromolecules* **28**, 8759 (1995).
22. I. Tinoco Jr., C. Bustamante, *Biophys. Chem.* **101-102**, 513 (2002).
23. The $\Delta x_{N \rightarrow U}^\ddagger$ and $\Delta x_{I \rightarrow N}^\ddagger$ values represent the average width of the potential energy for each state along the mechanical reaction coordinate (6, 26) and thus describe the extent of structural distortion necessary to cross a transition-state barrier. A correlation has been noted between a protein's structure and the position of the unfolding transition state: $\Delta x_{N \rightarrow U}^\ddagger$ appears to be large when the stabilizing interactions are predominantly long-range hydrophobic interactions, and small when they consist of clusters of short-range interstrand hydrogen bonds (6, 30). The value of 2 nm measured here for RNase H is on the higher end of the distribution of transition-state distances obtained for other proteins using the AFM (0.25 to 1.7 nm) [(26) and references therein].
24. M. Schlierf, H. Li, J. M. Fernandez, *Proc. Natl. Acad. Sci. U.S.A.* **101**, 7299 (2004).
25. E. Rhoades, M. Cohen, B. Schuler, G. Haran, *J. Am. Chem. Soc.* **126**, 14686 (2004).
26. C. Bustamante, Y. R. Chemla, N. R. Forde, D. Izhaky, *Annu. Rev. Biochem.* **73**, 705 (2004).
27. K. Kuwajima, *Proteins* **6**, 87 (1989).
28. G. M. Spudich, E. J. Miller, S. Marqusee, *J. Mol. Biol.* **335**, 609 (2004).
29. The I53D RNase H variant did not exhibit any low-force unfolding transitions; refolding occurred as a gradual compaction rather than as a single sharp transition, and hopping was not observed at any force examined. Refolding to the native state was qualitatively slower for the I53D variant, which suggests that the formation of the molten globule-like intermediate of RNase H speeds up the attainment of its folded state. This is consistent with bulk kinetic studies that suggest that folding can be accelerated if the interactions that stabilize the intermediate stabilize the transition state structure to an even greater extent (28).
30. H. Lu, K. Schulten, *Proteins* **35**, 453 (1999).
31. H. S. Chan, K. A. Dill, *Proteins* **30**, 2 (1998).
32. We thank R. Dahlquist for support and experimental advice in the early stages of this work, and the Marqusee and Bustamante labs for helpful discussions. Supported by NIH grants GM50945 (S.M.) and GM32543 (C.B.), U.S. Department of Energy grant AC03765f00098 (C.B.), NIH training grant GM008295 (E.A.S.), and a NSF predoctoral fellowship (E.A.S.).

Supporting Online Material

www.sciencemag.org/cgi/content/full/309/5743/2057/DC1
 Materials and Methods
 SOM Text
 Figs. S1 to S6

28 June 2005; accepted 17 August 2005
 10.1126/science.1116702

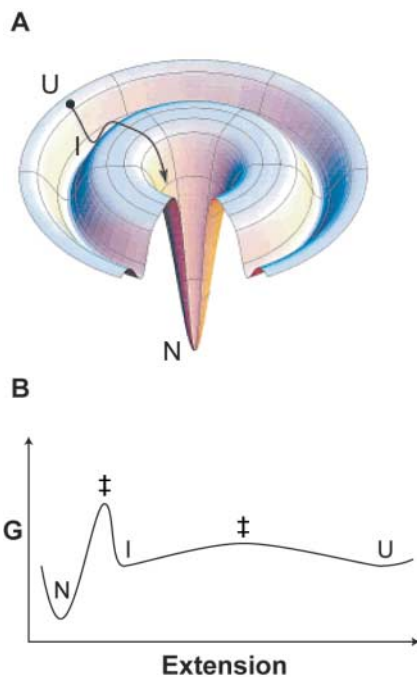


Fig. 4. The energy landscape of RNase H. (A) Schematic representation (31) of the energy landscape of RNase H depicting a reduction in conformational entropy as the protein folds through an on-pathway, obligatory, and productive intermediate species. (B) Free energy reaction profile of RNase H at ~5.5 pN, the force at which $\Delta G_{(U)} = 0$. Relative distances between states correlate with the values obtained experimentally (Fig. 2, A and B, and Fig. 3A), assuming that $\Delta x_{N \rightarrow U}^\ddagger$ obtained at a range of forces between 15 and 20 pN holds for this lower force.

References and Notes

1. P. S. Kim, R. L. Baldwin, *Annu. Rev. Biochem.* **59**, 631 (1990).
2. H. Roder, W. Colon, *Curr. Opin. Struct. Biol.* **7**, 15 (1997).
3. R. L. Baldwin, G. D. Rose, *Trends Biochem. Sci.* **24**, 77 (1999).
4. M. J. Parker, S. Marqusee, *J. Mol. Biol.* **293**, 1195 (1999).
5. M. S. Kellermayer, S. B. Smith, H. L. Granzier, C. Bustamante, *Science* **276**, 1112 (1997).
6. M. Rief, J. Pascual, M. Saraste, H. E. Gaub, *J. Mol. Biol.* **286**, 553 (1999).
7. R. B. Best, B. Li, A. Steward, V. Daggett, J. Clarke, *Biophys. J.* **81**, 2344 (2001).
8. A. F. Oberhauser, C. Badilla-Fernandez, M. Carrion-Vazquez, J. M. Fernandez, *J. Mol. Biol.* **319**, 433 (2002).
9. D. J. Brockwell *et al.*, *Nat. Struct. Biol.* **10**, 731 (2003).